

B. Colling, T. Eade, M.J. Joyce,
R. Pampin, F. Seyvet, A. Turner, V. Udintsev

Neutronics Analysis for Integration of ITER Diagnostics Port EP10

Enquiries about copyright and reproduction should in the first instance be addressed to the Culham Publications Officer, Culham Centre for Fusion Energy (CCFE), Library, Culham Science Centre, Abingdon, Oxfordshire, OX14 3DB, UK. The United Kingdom Atomic Energy Authority is the copyright holder.

Neutronics Analysis for Integration of ITER Diagnostics Port EP10

B. Colling^{1,2}, T. Eade¹, M.J. Joyce²,
R. Pampin³, F. Seyvet³, A. Turner¹, V. Udintsev⁴

¹*CCFE, Culham Science Centre, Abingdon, Oxon OX14 3DB, United Kingdom*

²*Department of Engineering, Lancaster University, Lancashire, LA1 4YR, UK*

³*Fusion for Energy, Josep Pla 2, Torres Diagonal Litoral B3, 08019 Barcelona, Spain*

⁴*ITER Organization, Route de Vinon-sur-Verdon, CS 90 046, 13067 St. Paul Lez Durance Cedex, France*

The following article appeared in a special edition of the International Journal “Fusion
Engineering and Design”.

Further reproduction distribution of this paper is subject to the journal publication rules.

Neutronics Analysis for Integration of ITER Diagnostics Port EP10

Bethany Colling^{a,b}, Tim Eade^a, Malcolm J. Joyce^b,
Raul Pampin^c, Fabien Seyvet^c, Andrew Turner^a, Victor Udintsev^d

^a Culham Centre for Fusion Energy, Culham Science Centre, Abingdon, Oxon, OX14 3DB, UK

^b Department of Engineering, Lancaster University, Lancashire, LA1 4YR, UK

^c Fusion for Energy, Josep Pla 2, Torres Diagonal Litoral B3, 08019 Barcelona, Spain

^d ITER Organization, Route de Vinon-sur-Verdon, CS 90 046, 13067 St. Paul Lez Durance Cedex, France

Shutdown dose rate calculations have been performed on an integrated ITER C-lite neutronics model with equatorial port 10. A fully shielded configuration, optimized for a given diagnostic designs (i.e. shielding in all available space within the port plug drawers), results in a shutdown dose rate in the port interspace, from the activation of materials comprising equatorial port 10, in excess of 2000 $\mu\text{Sv/h}$. Achieving dose rates of 100 $\mu\text{Sv/h}$ or less, as required in areas where hands-on maintenance can be performed, in the port interspace region will be challenging. A combination of methods will need to be implemented, such as reducing mass and/or the use of reduced activation steel in the port interspace, optimization of the diagnostic designs & shielding of the port interspace floor. Further analysis is required to test these options and the ongoing design optimization of the EP10 diagnostic systems.

Keywords: ITER, neutronics, diagnostic port, shutdown dose rate, MCNP

1. Introduction

The ITER Nuclear Facility INB-174 will include a number of diagnostic systems to provide measurements necessary to control, evaluate and optimize plasma performance. The diagnostic systems require direct access to the plasma which is facilitated by housing them within a number of ports and port plugs provided in the design of the vacuum vessel. This work concerns the diagnostic equatorial port 10 (EP10).

EP10 contains four diagnostic systems: the edge core Thomson scattering (ETS), the poloidal polarimetry (POPOLA), the core plasma Thomson scattering (CPTS) and the plasma position reflectometry (PPR), systems. These diagnostic systems are housed in an equatorial port interspace and generic diagnostic equatorial port plug (DEPP). The generic DEPP consists of a frame, diagnostic first wall (DFW), diagnostic shield module (DSM), a closure plate, neutron stoppers and three diagnostic drawers.

The diagnostic systems will be subject to significant neutron irradiation as a result of the direct plasma access. Neutron irradiation leads to a number of effects within the materials, including nuclear heating, material damage, helium production and material activation. Activation of materials can pose a radiological hazard to personnel during shutdown when access to the port interspace may be required for maintenance. ITER Project Requirements [1] call for a design that ensures the shutdown dose rate (SDDR), in areas where in-situ maintenance activities are foreseen, be as low as reasonably achievable (ALARA) and shall not exceed 100 $\mu\text{Sv/h}$ at 10^6 s after shutdown without formal project approval [PR1782-R].

An understanding of the distribution of nuclear fields throughout the port plug and port interspace region of an integrated EP10 neutronics model is required to facilitate

design progression with suitable shielding. It should be noted that the diagnostic systems in EP10 are in the pre-conceptual design stage, except for the PPR which is further on in the design process. And, that other studies on the design of the diagnostics are ongoing with an aim to reduce the SDDR.

In this work neutronics analysis has been performed in order to compute the SDDR in the EP10 port interspace region for a number of shielding arrangements and a closed plug.

2. EP10 Neutronics Model

A neutronics model of EP10 has been created, via the simplification of CAD models and conversion to MCNP (using MCAM [2]). This model was subsequently integrated into the C-lite ITER neutronics model along with representations of the neighboring ports.

Variations of the MCNP EP10 C-lite model were created with different shielding arrangements within the port plug drawers and between the back of the drawers and the port plug closure plate (see Fig. 1):

- 'Baseline' model with shielding added to the area between the drawers and closure plate
- 'Closed plug' model with all penetrations effectively closed off by filling the drawers with shielding
- 'Open POPOLA drawer' model with penetrations in the other two drawers filled with shielding
- 'Fully shielded' model, an optimized arrangement with shielding in all available space within the port plug

The shielding material (referred to from herein as simply B4C) has been modelled as a homogenous mix of boron carbide and 5% (by volume) stainless steel SS316L(N)-IG. The mass density of the B4C shielding

has been adjusted in each model to represent differing packing fractions in order to ensure the maximum weight limit of the port plug is not exceeded.

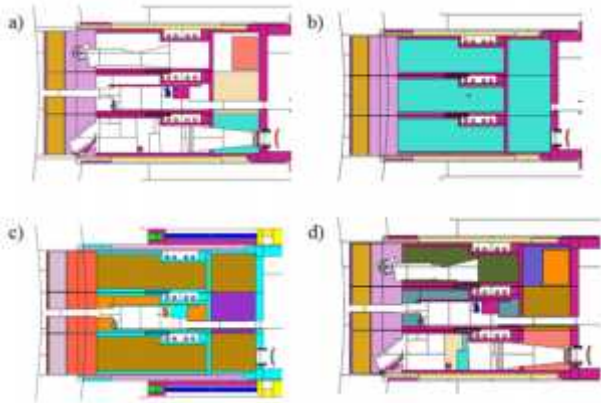


Fig. 1. Cross section plot through EP10 at a height of 60cm, showing the different shielding arrangements in each of the three drawers.

2.1 Port interspace materials

The materials within the port interspace region of EP10 (Fig. 2) comprise of the diagnostic components and associated structural equipment (i.e. trolley frame). In this work, it is conservatively assumed that the materials within the port interspace may not be subject to the same restrictions on impurities as those within the port plug. The majority of the steel within the interspace has therefore been modelled as stainless steel 316L with Co and Nb mass content at 0.2% and 0.1% respectively. Low activation steel (stainless steel 316L(N) ITER grade) has been used within the port plug.

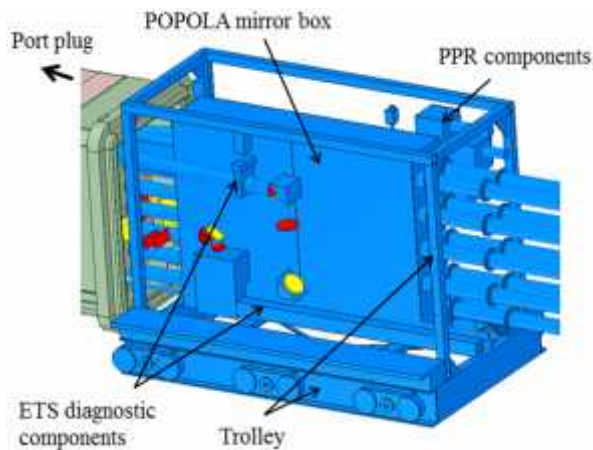


Fig. 2. View of the port interspace components from the side of the ETS drawer. Components in blue are steel. The red and yellow are lenses and mirrors respectively.

An estimation of the steel mass within the port interspace has been calculated as 12.8 tonnes, using the volume of the steel components within the simplified CAD model and assuming a mass density of 7.93 g/cm³; no mass density corrections for simplification of the CAD has been taken into account. The trolley frame contributes the majority of the mass at ~ 9 tonnes.

3. Neutronics Analysis

3.1 Analysis method

In order to compute the SDDR, neutron and photon transport is required and a method for calculating the material activation to produce a shutdown photon source. The Rigorous-2-Step (R2S) method [3] has been used, and can be broken down into the following stages:

- Calculate neutron spectra over a 3-D mesh (performed using MCNP with the standard 500 MW ITER 40 degree plasma source [4] with an intensity of 1.9718×10^{19} neutrons/second);
- For each mesh voxel perform an activation calculation;
- From the activation calculation results derive a shutdown photon source for a 10^6 s decay time;
- Collate the individual photon sources into a 3-D MCNP decay photon source definition;
- Use the derived shutdown source in a subsequent photon transport calculation to determine the shutdown dose rate at 10^6 seconds.

The R2S method is implemented at CCFE using the MCR2S-II code [5] which couples an MCNP 3-D rectangular mesh tally with the inventory code FISPACT-II [6], in order to produce a shutdown photon source which can be read using a custom source routine in MCNP.

For local¹ activation calculations two mesh tallies are used, one covering the port plug region and one over the port interspace. In the case of global² activation calculations, for the fully shielded model, six mesh tallies are used to cover the majority of the 40 degree sector model. It should be noted that the coverage of the port plug and port interspace mesh for the fully shielded model differs slightly to accommodate the six meshes.

The replacement of major components within EP10 is not foreseen and therefore use of the full SA2 safety plasma irradiation scenario is conservative and has been applied to all components within each mesh.

3.2 Simulation codes and nuclear data

The particle transport code MCNP6.1 [7] has been used to perform neutron transport simulations and the photon shutdown dose rate calculations. The FENDL2.1 [8] neutron cross section data has been used and where unavailable, ENDF-B-VII [9]. For photon cross section data, the MCPLIB84 data library has been used. Activation calculations have been performed using FISPACT-II with the EAF-2010 [10] activation data.

¹ Local activation refers to the activation of the materials comprising EP10 and the near vicinity, covered by the port plug and port interspace meshes. This activation is still as a result of global neutron transport.

² Global activation refers to the activation of materials covered by all 6 meshes, i.e. the majority of the 40 degree sector model.

3.3 Global variance reduction

The scale and complexity of the neutronics model requires the use of variance reduction techniques to provide results with sufficiently low variance within an acceptable time frame. A global variance reduction technique [11] has been used to generate neutron weight windows for the analyses documented in this paper. The weight window has two energy bins 0-0.1 MeV and 0.1-20 MeV and a spatial resolution of approximately 10 cm.

4. Results and Discussion

4.1 Baseline model

The SDDR, computed from the global neutron transport and local activation of EP10 using the ‘baseline shielding arrangement was shown to be in the 10’s of thousands of $\mu\text{Sv/h}$ in the port interspace; considerably higher than the 100 $\mu\text{Sv/h}$ limit for hands-on maintenance. There is little material within the port drawers (Fig. 1a) to attenuate neutrons and it is therefore evident that a considerable amount of additional shielding is required, along with optimization of the diagnostic designs. Neutronics analysis on the shielding within the three drawers provides an important stage in the optimization process.

4.2 Closing the penetrations

By filling all penetrations and optical paths with B4C shielding to create an effectively closed plug, the SDDR contribution from neutron streaming in the port plug gaps and neighboring systems can be computed. The SDDR_{R1} ³ (again from local activation of EP10) is approximately 1260 $\mu\text{Sv/h}$; a significant reduction from the ‘baseline’ model but still not below the 100 $\mu\text{Sv/h}$ requirement (Fig. 3).

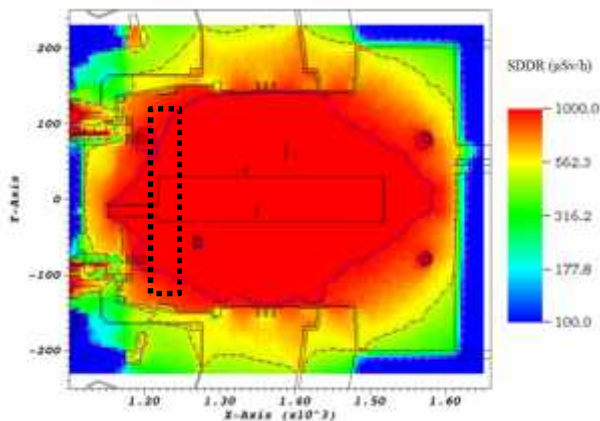


Fig. 3. SDDR in a horizontal slice (height of 60 cm) of the EP10 port interspace with a closed port plug. Contour lines for 100 $\mu\text{Sv/h}$, 500 $\mu\text{Sv/h}$ and 1000 $\mu\text{Sv/h}$ are presented by the pink dashed line, brown dot/dashed line and the blue dotted line respectively. Location of the R1 standard tally region shown by the black dashed rectangular box.

³ R1 refers to a standard tally adopted within the fusion community for ITER port plug analysis. SDDR_{R1} values are averaged over a rectangular box volume in the port interspace behind the closure plate (see Fig. 3).

The majority (~90%) of the SDDR_{R1} is due to the activation of material within the port interspace. Some of this material i.e. the diagnostic components and associated structural material (see Fig. 2) will be removed for maintenance procedures at some time after shutdown. Repeating the SDDR calculation without the activation from the removed materials results in a lower SDDR_{R1} of ~450 $\mu\text{Sv/h}$ (Fig. 4). It should be noted that removal of the interspace components will require remote handling if the SDDR is above the limit for hands on maintenance.

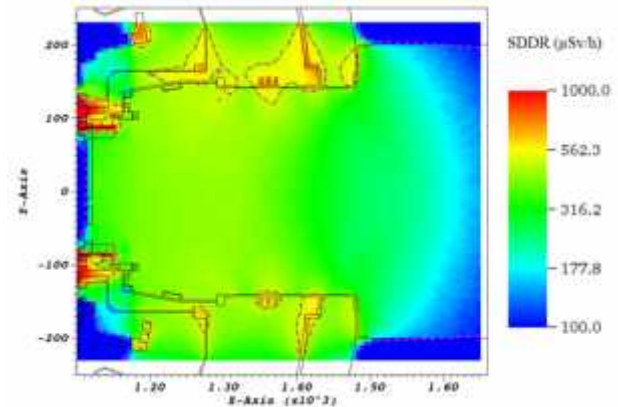


Fig. 4. SDDR in a horizontal slice (height of 60 cm) with diagnostic equipment removed from the interspace. Contour lines for 100 $\mu\text{Sv/h}$, 500 $\mu\text{Sv/h}$ and 1000 $\mu\text{Sv/h}$ are presented by the pink dashed line, brown dot/dashed line and the blue dotted line respectively.

4.3 The POPOLA drawer

Local activation SDDR calculations performed on a version of the EP10 C-lite neutronics model with the fully shielded POPOLA diagnostics drawer included, but the other two drawers effectively closed off, resulted in a SDDR_{R1} of 2070 $\mu\text{Sv/h}$; an increase of ~70% on the closed plug model results.

The current design of the POPOLA diagnostic optical paths does not allow for significant additional shielding within the port plug drawer, creating a significant streaming path. It is expected that this contribution to the port interspace SDDR will be significantly reduced through future design optimization of the POPOLA diagnostics.

4.4 Fully shielded plug- an optimized model

For the case of the ‘fully shielded’ EP10 C-lite neutronics model, where all available space within the drawers has been filled with B4C shielding (leaving only the diagnostic equipment and required penetrations for the optical paths), the resulting SDDR_{R1} from local EP10 activation is 2670 $\mu\text{Sv/h}$. Although an optimized shielding scenario has reduced the SDDR considerably, when compared to the baseline model results, it is more than double the closed plug scenario (see Fig. 5).

The SDDR contributions from the activation of neighboring systems were also calculated with the ‘fully shielded’ EP10 C-lite neutronics model. The

contribution from global activation increases the $SDDR_{R1}$ by $\sim 2.5\%$. The highest contributor, of the neighboring ports, is the LP. The activation of the LP results in a SDDR within the EP10 port interspace region of approximately 30 – 140 $\mu\text{Sv/h}$ (see Fig. 7). The neutron cross talk from the LP can be seen in Fig. 6.

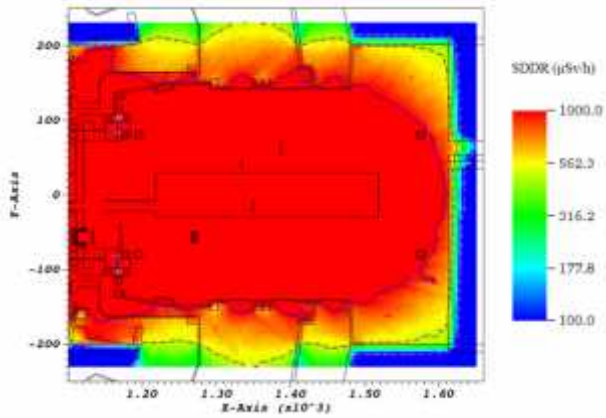


Fig. 5. Horizontal plot at a height of 60 cm showing the SDDR in the EP10 port interspace with a fully shielded plug. Contour lines for 100 $\mu\text{Sv/h}$, 500 $\mu\text{Sv/h}$ and 1000 $\mu\text{Sv/h}$ are presented by the pink dashed line, brown dot/dashed line and the blue dotted line respectively.

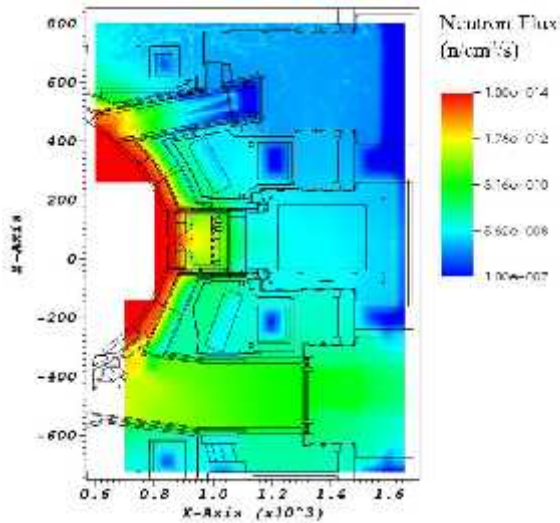


Fig. 6. Total neutron flux map in a vertical slice through the POPOLA drawer (at $PY = 0\text{cm}$)

Approximately 70% of the $SDDR_{R1}$, from local EP10 activation, is due to the activation of the port interspace materials. Removing the diagnostic equipment and associated structural material within the port interspace from the activation calculation, to simulate the removal of the material after shutdown, and repeating the SDDR calculation results in a reduced $SDDR_{R1}$ of $\sim 780 \mu\text{Sv/h}$. The contribution to the SDDR in the EP10 port interspace from the LP increases when the interspace diagnostic equipment is removed. This increase is thought to be due to the removal of shielding effects from the port interspace diagnostic equipment.

The diagnostic equipment within the interspace region is also shown to have a shielding effect on the

contribution to SDDR from the activation of the surrounding interspace structure i.e. the port interspace walls and floor. Removing the interspace diagnostic equipment increases the $SDDR_{R1}$ contribution from the surrounding interspace structure (Fig. 7 and Fig. 8) from approximately 270 $\mu\text{Sv/h}$ to 340 $\mu\text{Sv/h}$.

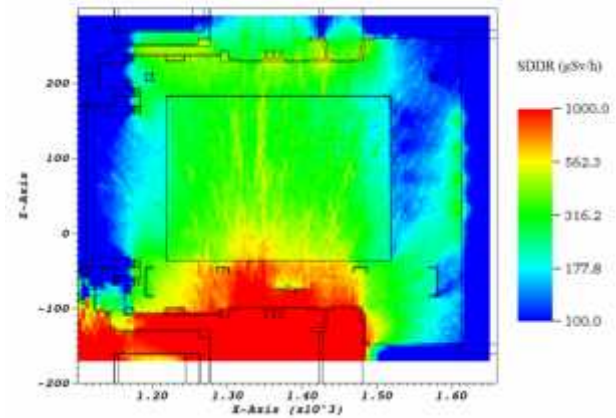


Fig. 7. SDDR in the EP10 port interspace from the activation of the LP and surrounding port interspace structures. A vertical slice through the POPOLA drawer ($PY = 0\text{cm}$).

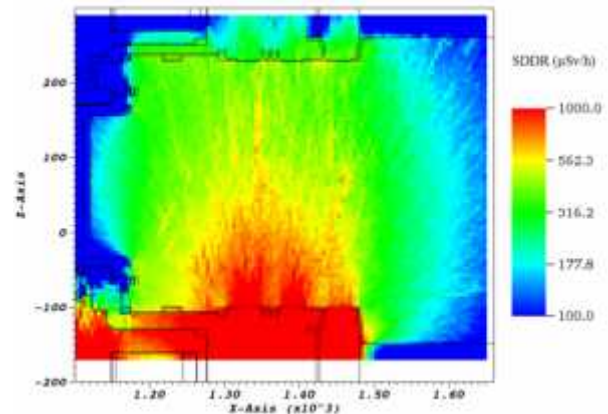


Fig. 8. SDDR in the EP10 port interspace from the activation of the LP and surrounding port interspace structures with the diagnostic equipment removed from the port interspace. A vertical slice through the POPOLA drawer ($PY = 0\text{cm}$).

4.5 Statistical uncertainty

Error propagation through a R2S calculation is an active area of research. For the work presented in this paper a significant amount of computational effort was used to reduce the statistical uncertainties on the neutron and gamma transport steps.

The relative statistical uncertainty, associated with the photon transport calculations, is below 5% for all values quoted in this paper. For the SDDR maps presented, the relative statistical uncertainty is below 5-10% in the majority of the areas of importance for this port interspace analysis. Where data has been post processed as a summation of two or more tally results, the statistical uncertainties have been added in quadrature.

5. Conclusions & Recommendations

1. The EP10 port plug with a ‘fully shielded’ scenario results in a $SDDR_{R1}$ of 2670 $\mu\text{Sv/h}$ at 10^6 s after shutdown; increasing by $\sim 2.5\%$ when the contribution from global activation is included. This is more than an order of magnitude greater than the 100 $\mu\text{Sv/h}$ project requirement for hands-on maintenance.

2. The majority of the SDDR in the interspace region of the ‘fully shielded’ scenario was calculated to originate from the activation of the interspace diagnostic equipment (approximately 70-80%). If the activation of this equipment can be reduced to a negligible value, e.g. by removing mass and/or using low activation materials (in line with the Project Requirements, PR1478-R [1]), the $SDDR_{R1}$ can be expected to lie between ~ 450 $\mu\text{Sv/h}$ and ~ 780 $\mu\text{Sv/h}$ (results from the ‘closed plug’ and ‘fully shielded’ models respectively, with interspace components removed).

3. When considering the contribution from the neighboring ports, the LP provides the highest contribution to the SDDR in the port interspace, approximately 1 - 6 % of the global total. This contribution is increased when the materials compromising the port interspace diagnostic equipment are removed. Therefore consideration should be given to shielding the floor of the EP10 interspace to reduce the SDDR contribution from the LP and the neutron cross talk.

Table 1. Summary of $SDDR_{R1}$ values for the different shielding arrangements

EP10 Neutronics Model	$SDDR_{R1}$ ($\mu\text{Sv/h}$)
Closed plug	~ 1260
Closed plug with port interspace equipment removed	~ 450
Open POPOLA drawer	~ 2070
Fully shielded	~ 2670
Fully shielded with port interspace equipment removed	~ 780

It is clear, from the results presented, that reducing the SDDR in the port interspace region of EP10 will be challenging, and that there is not just one single element that can be changed in order to achieve dose rates of 100 $\mu\text{Sv/h}$ or less. It is however expected that once the design is optimized the SDDR will be significantly reduced.

If the neutron streaming through the port plug can be made negligible (i.e. as close to the ‘closed plug’ model as possible) and the contribution from the interspace diagnostic equipment reduced to a negligible value (i.e. similar to a closed plug with the interspace components removed), the $SDDR_{R1}$ would still be approximately 450 $\mu\text{Sv/h}$. A combination of methods for reducing the SDDR will need to be implemented. For example,

further reductions in the SDDR could be achieved by reducing the global leakage of the neutrons outside of the vacuum vessel, B4C lining of the bioshield, improved LP shielding and reduced gap streaming etc. Further analysis is required to test these options and ongoing design optimization of the EP10 diagnostics.

Acknowledgments

This work was carried out using an adaptation of the C-lite MCNP model which was developed as a collaborative effort between the FDS team of INEST China, University of Wisconsin-Madison, ENEA Frascati, CCFE UK, JAEA Naka, and the ITER Organization.

This work was funded by F4E under contract F4E-OMF-466-01-01. The views and opinions expressed herein do not necessarily reflect those of F4E or the ITER Organization. F4E is not liable for any use that may be made of the information contained herein. The author would like to thank the following organizations for additional funding support: Lancaster University, the European Union's Horizon 2020 research and innovation programme and the RCUK Energy Programme [grant number EP/I501045].

To obtain further information on the data and models underlying this paper, please contact PublicationsManager@ccfe.ac.uk.

References

- [1] S. Chiocchio et al, ITER Project Requirements, Private Communication
- [2] Y. Wu, FDS Team, CAD-based interface program for fusion neutron transport simulation, *Fusion Engineering and Design* 84 (2009) 1987-1992
- [3] Y. Chen et al., *Fusion Engineering and Design* 63–64 (2002), p107.
- [4] E. Polunovskiy, SDEF card for the ITER standard neutron source (inductive operation scenario with 500MW of fusion power), IDM UID - ITER_D_2KS8CN v1.4, June 2006.
- [5] A. Davis and R. Pampin, *Fus. Eng. Des.* 85 (2010) p87.
- [6] JC. Sublet, ‘The FISPACT-II User Manual’, CCFE-R(11)11 Issue 6, June 2014.
- [7] D. Pelowitz et al. MCNP6 Users’ Manual – Code Version 1.0, LA-CP-13-00634 Rev 0, May 2013.
- [8] D. Lopez Al-dama and A. Trkov, ‘FENDL-2.1: update of an evaluated nuclear data library for fusion applications’, IAEA Report INDC(NDS)-46, 2004.
- [9] M.B. Chadwick et al. ENDF/B-VII.1: Nuclear Data for Science and Technology: Cross Sections, Covariances, Fission Product Yields and Decay Data”, *Nucl. Data Sheets* 112(2011)2887.
- [10] JC. Sublet, EAF 2010 neutron-induced cross section library, CCFE-R(10)05, April 2010.
- [11] A. Davis and, A. Turner, Comparison of global variance reduction techniques for Monte Carlo radiation transport simulations of ITER, *Fus. Eng. Des.* 86, Issues 9–11, October 2011, Pages 2698-2700.